

The Use of Experimental Design to Study the Responses of Continuous Devulcanization Processes

P. Sutanto, F. Picchioni, L. P. B. M. Janssen

Chemical Engineering Department, University of Groningen, Nijenborgh, AG Groningen, The Netherlands

Received 23 March 2006; accepted 25 June 2006

DOI 10.1002/app.25022

Published online in Wiley InterScience (www.interscience.wiley.com).

ABSTRACT: This paper presents the use of statistical analysis for studying the responses of two continuous devulcanization processes (of the EPDM roofing sheet and the EPDM profile) in the extruder. The response is represented by the reaction conversion, which is denoted as the relative decrease in crosslink density. Experimental design is considered as a useful tool when the kinetic data for the physical modeling are not available. The models derived

show similar tendency of both processes with respect to the temperature and the screw speed. A difference is observed in their responses to the feed rate, which might be the consequence of their different devulcanization rates. © 2006 Wiley Periodicals, Inc. *J Appl Polym Sci* 102: 5028–5038, 2006

Key words: recycling; rubber; processing; ethylene–propylene–diene monomer; extrusion; modeling

INTRODUCTION

EPDM is the fastest growing elastomer among the synthetic rubbers since its introduction in 1963.^{1–4} It represents 7% of the world rubber consumption and it is the most widely used nontire rubber. The main use of EPDM (over a third of its global output)⁴ is in automotive applications such as profiles, hoses, and seals; in building and construction as profiles, roofing foil, and seals; in cable and wire as insulation and jacketing. EPDM is also used in blends with general-purpose rubbers to improve the ozone and weathering resistance in products such as in cover strips and thermoplastic material used for exterior automotive applications (bumpers and panels).² Contrary to the other rubber parts of cars, namely tires, EPDM rubber has received much less attention concerning the recycling issue.

Current researches on EPDM devulcanization have involved the use of an extruder. An investigation into the ultrasonic devulcanization of sulfur-cured EPDM rubber was conducted by Yun et al.^{5–7} An ultrasonic device is mounted in the gap between the horn and the die plate of the extruder. The EPDM vulcanizate was loaded into the hopper. The extruder is in this case used to convey and compress the

EPDM vulcanizate to the devulcanization zone. The ultrasonic treatment of the rubber occurred in the gap between the horn and the die plate of the reactor. Gap size and ultrasonic amplitude were processing parameters and had an influence on the degree of devulcanization. An increase of the ultrasonic amplitude and a decrease of the gap size increased the degree of devulcanization of EPDM.

Toyota developed a technology for continuously reclaiming EPDM rubber within a short time (10 min), using a twin screw reactive extruder.^{8–12} The continuous devulcanization processing using the extruder was made possible by optimizing the various conditions, which include the reaction temperature, screw geometry, and rotational speed, and the amounts of additives such as devulcanizing agent and reclaiming oil.

The previous work of van Duin et al.¹³ on the devulcanization agent for EPDM has shown the effectiveness of amine. The devulcanization process at high temperatures is assumed to have a radical character, and amines might facilitate this reaction. It was also shown that the use of these amines reduced the crosslink density mainly by crosslink scission, producing revulcanizable rubber.¹³

In this research, the use of shear is combined with the use of α -H aliphatic amines as devulcanizing agent to obtain revulcanizable EPDM rubbers. To achieve a feasible EPDM devulcanization, the process parameters in the extruder, such as the shear stress, the temperature, and the screw configuration, have to be optimized.

Experimental design is a useful tool to study the process response for a quick test when the kinetic data are not available. Since any reactions occur

Correspondence to: L. P. B. M. Janssen (L.P.B.M.Janssen@rug.nl).

Contract grant sponsors: Technology Foundation STW, Applied Science Division of the Dutch Scientific Foundation NWO; DSM Elastomers B.V.; Hertel B.V.; Rhein Chemie Rheinau GmbH; Rubber Resources B.V.

according to a particular kinetic equation or physical phenomenon, a process will follow certain tendencies. These tendencies are to be observed by the experimental design method, resulting in a statistical model showing the correlation between the input(s) and output(s).

Building an adequate model for an extrusion process requires knowledge of the reaction kinetics and physical properties of the material during its transport in the extruder. Deriving a kinetic model as has been discussed in our previous research^{14,15} and introducing it in the reactive extrusion system might be a laborious method for practical application. Therefore, another approach is adopted here, i.e., using the statistical analysis for studying the continuous devulcanization in the extruder.

METHODOLOGY

Considering the complexities in modeling the devulcanization process in the extruder, another approach was proposed. The extruder is considered as a black box as in Figure 1, where the rubber feed rate, screw speed, and temperature are the only important input variables. The output of this black box is characterized by the degree of devulcanization, which can be calculated from its relative crosslink density.

Other operating parameters in the extruder such as residence time, heat transfer rate, shear force, reaction rate are included indirectly in the model, since their values are affected by the variables taken into account, i.e., the three input variables. The devulcanization of EPDM requires a devulcanizing agent, namely hexadecylamine (HDA) is used in this research.¹³ Its concentration was varied for the roofing sheet material, but was set at its optimum for the profile material, i.e. 3×10^{-4} mol/g rubber (=72.3 g HDA/kg rubber) according to the result from screening experiments. The use of higher concentration above this value is undesired in industrial application, due to the high cost.

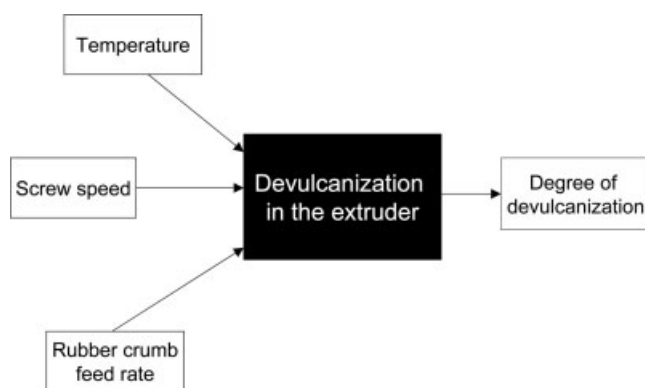


Figure 1 Simplified model: black box model.

It should be kept in mind that the model produced in this way is representative only in the ranges studied and therefore extrapolating the equation might lead to a large error. The statistical model is useful as a quick method in studying the influence and the significance of each of the parameters. Optimization of the process can then be done effectively by adjusting these significant parameters.

The strategy in designing the experiments for this statistical method is summarized as follows:

1. estimate which parameters might have a significant influence on the process, which can be done by doing screening experiments in a batch system;
2. design an experimental series containing all these parameters at several levels;
3. analyze the experimental results by means of analysis of variance (ANOVA) to determine whether the parameters studied and their interactions have a significant influence on the process;
4. derive a statistical model that can represent the behavior of the process in the range studied;
5. validate the model;
6. optimize the process within this range.

EXPERIMENTAL

Material and equipments

Two types of EPDM materials were examined, i.e., the production waste for building profile material and roofing sheet (both produced by Hertel B.V.). The building profile material contains Keltan 4703, 110 phr carbon black, and an accelerator/sulfur ratio of 8.6 : 1 (efficient-vulcanized); the roofing sheet contains Keltan 720, 73 phr carbon black, and an accelerator/sulfur ratio of 1.5 : 1 (semiefficient-vulcanized). Both materials were cut into crumbs of smaller than 1 cm using a rubber shredder.

The experimental setup for the devulcanization in the extruder is depicted in Figure 2. The rubber crumb is fed to the corotating twin screw extruder by a hopper. The feed inlet is flushed by N₂, preventing air coming into the extruder to minimize the oxidation reactions. The amine (HDA) is melted at 100°C and is fed as a liquid into the extruder. The rubber crumbs, oil, and amine pass through the mixing zone before entering the reaction zone. In the mixing zone, the kneading elements are mounted in a negative stagger angle to improve mixing. Negative staggered-mounted kneading section gives a negative transporting action, holding the material back to the feeding section until the pressure build up is high enough to overcome this. In the reaction zone, high shear rate and high devulcanization tem-

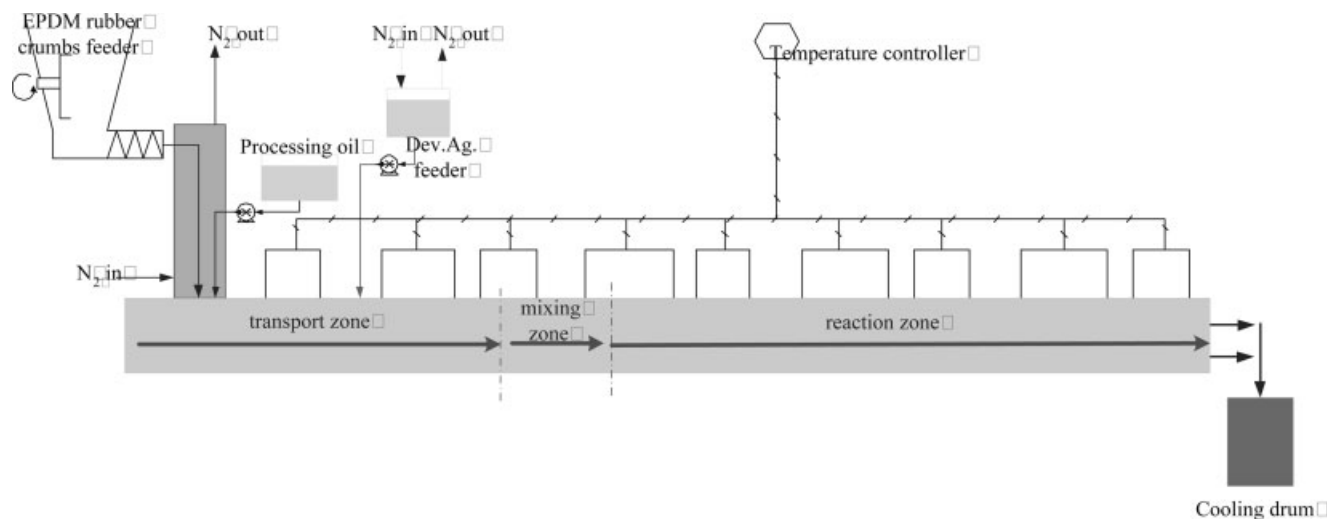


Figure 2 The extruder setup for the continuous devulcanization process.

perature (between 230 and 300°C) are applied to the mixture.

Screw configuration is as such designed so that it provided enough time (10–20 min at the investigated flow rate) for the devulcanization to occur in the range of feed rates studied.

Samples were taken after a steady state is reached, which could be observed from steady pressure and temperature values. After steady conditions are reached, the sample can be taken after waiting for a certain time, which is the estimated residence time of the rubber in the extruder. The estimated residence time varies between experiments, depending on the feed rate and screw speed.

Analytical methods

Swelling test is used here as an indication of the degree of devulcanization. The test was conducted by swelling the sample in decaline, weighing the swollen sample, drying the sample in a vacuum oven, and weighing the dried sample consecutively. The crosslink density is subsequently calculated using Flory–Rehner equation.¹⁶

EPDM PROFILE MATERIAL

Experimental design

Two-level factorial design¹⁷ was applied here to find the effects of each input variable and/or the combinations of them on the degree of devulcanization. Three input variables were considered, namely the screw speed, rubber feed rate, and temperature.

The number of combinations needed for a full factorial design for three variables is $2^3 = 8$ experiments. The variables were set either to their high value or to their low value. The low value is coded

as -1 and the high as 1 (Table I). A total of 16 experiments were performed to test the eight combinations in duplo, which in turn reduces the error of the model.

When the design factors are quantitative, a model can be built in the following form:

$$\text{Degree of decrosslinking} = f_a A + f_b B + f_c C + f_{ab} AB + f_{ac} AC + f_{bc} BC + f_{abc} ABC + \text{Intercept} \pm \text{Error} \quad (1)$$

where f 's are the coefficient of each factor or of their interactions.

Results and discussion

Analysis of variance

The results of the experiments are presented in Table II. Decrosslinking degree and HDA consumption are calculated as

$$\text{Decrosslinking degree} = \frac{XL_0 - XL_{\text{end}}}{XL_0} \times 100\% \quad (2)$$

It can be seen from the results that the decrosslinking degree varies between the combinations. ANOVA was made to see which factors play major roles in

TABLE I
Settings for Full Factorial Design

| Parameter | Code | High (1) | Low(-1) |
|-------------------|------|----------|---------|
| Feed rate (kg/h) | A | 7 | 3 |
| Screw speed (rpm) | B | 200 | 50 |
| Temperature (°C) | C | 300 | 250 |

TABLE II
Results of the Factorial Experiments

| Experiment | Flow rate (kg/h) | Screw speed (rpm) | T (°C) | Decrosslinking degree (%) |
|------------|------------------|-------------------|--------|---------------------------|
| 1 | 3 | 50 | 250 | 58.1 |
| 2 | 3 | 50 | 250 | 57.4 |
| 3 | 3 | 50 | 300 | 78.0 |
| 4 | 3 | 50 | 300 | 79.4 |
| 5 | 3 | 200 | 250 | 65.4 |
| 6 | 3 | 200 | 250 | 68.6 |
| 7 | 3 | 200 | 300 | 78.0 |
| 8 | 3 | 200 | 300 | 78.4 |
| 9 | 7 | 50 | 250 | 58.6 |
| 10 | 7 | 50 | 250 | 57.6 |
| 11 | 7 | 50 | 300 | 75.0 |
| 12 | 7 | 50 | 300 | 75.4 |
| 13 | 7 | 200 | 250 | 63.7 |
| 14 | 7 | 200 | 250 | 64.8 |
| 15 | 7 | 200 | 300 | 75.5 |
| 16 | 7 | 200 | 300 | 75.4 |

the process. The result of ANOVA on the degree of decrosslinking as the dependent variable is listed in Table III.

As shown in Table III, the *P*-values of the flow, rpm, temperature, and rpm × *T* interaction are lower than 0.005, confirming that their effects on the decrosslinking degree are significant; while that of the other (interaction), factors are negligible.

Regression model

Regression of eq. (1) was done in Statistica® and the equation constants are listed in Table IV for decrosslinking degree, containing only the significant factors.

The predicted decrosslinking degrees calculated by this model are plotted against the experimental observed values in Figure 3, resulting in an *R*² value of 0.99. The *R*² value is an indication of the goodness of fit of the model; in this case, it shows that 99% of the variation in decrosslinking degree can be explained by the model.

TABLE III
Analysis of Variance for Each Factor and Their Interactions on the Decrosslinking Degree

| Factor | SS | DoF | MS | <i>P</i> -value |
|-----------------------|----------|-----|--------|-----------------|
| <i>T</i> | 0.091327 | 1 | 0.0913 | 0.00000 |
| RPM | 0.005730 | 1 | 0.0057 | 0.00006 |
| Flow | 0.001880 | 1 | 0.0019 | 0.00227 |
| <i>T</i> × RPM | 0.006111 | 1 | 0.0061 | 0.00005 |
| <i>T</i> × Flow | 0.000368 | 1 | 0.0004 | 0.08691 |
| Flow × RPM | 0.000144 | 1 | 0.0001 | 0.25681 |
| Flow × <i>T</i> × RPM | 0.000353 | 1 | 0.0004 | 0.09260 |
| Error | 0.000775 | 8 | 0.0001 | |
| Total | 0.106688 | 15 | | |

According to the model derived, the maximum degree of decrosslinking that can be achieved was found at the boundary of the range investigated, i.e., 300°C and 200 rpm, with a value of 80% decrosslinking degree.

From the model derived, a 3-D plot and a contour plot were prepared in Matlab® by setting the flow rate at a constant value of 3 kg/h. The flow rate is set at its low value since the decrosslinking degree is negatively influenced by the flow rate, according to the equation, and therefore, the maximum decrosslinking degree in the range studied is reached at the low setting of the flow rate.

The 3-D plot in Figure 4 shows the surface response of the model as a function of screw speed and temperature. The response does not show any peak/optimum point, but it shows a bend on the surface. By increasing the screw speed at low temperature, a significant increase of the conversion is observed, while increasing it at high temperature hardly affects the decrosslinking rate.

At high temperature, the effect of shear is less significant than at low temperature because of a rapid decrease of viscosity with the increase of temperature. The shear stress is a function of shear rate and viscosity; therefore, when the viscosity is lower,

TABLE IV
List of the Coefficient Values in Eq. (1)

| | Value |
|--------------------------------------------------|----------------------------|
| Intercept | -0.50045 |
| Flow rate (kg/h), <i>f_a</i> | -0.00542 |
| Screw speed (rpm), <i>f_b</i> | 0.0031186 |
| Temperature (°C), <i>f_c</i> | 0.0043249 |
| Temperature × Screw speed, <i>f_{bc}</i> | -1.0423 · 10 ⁻⁵ |
| Error (+/-) | 0.00246 |

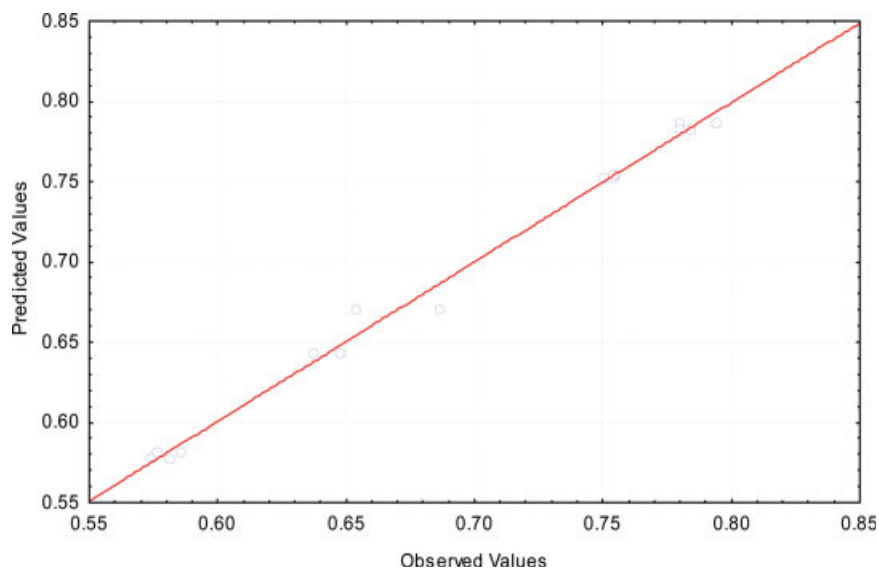


Figure 3 Model-predicted values versus observed values of the decrosslinking degree. [Color figure can be viewed in the online issue, which is available at www.interscience.wiley.com.]

the change of shear stress with shear rate is less significant.

For practical applications, a contour plot (Fig. 5) showing isolines is a useful tool to determine the operating conditions required to obtain a certain conversion. From this plot, the corresponding screw speed and temperature required to reach a certain degree of decrosslinking can be easily read.

Model validation

The next step of the statistical modeling is checking the predictive power of the model within the range studied and, if it is desired, the extensibility of the

model. Figure 6 shows the validation results of the model. Figure 6 shows the validation results of the model. The diamond points are the results from experiments in the range studied (inside the boundaries in Table I), while the square points (numbered) are from experiments done outside the boundaries studied. Table V shows the conditions of the experiments outside the flow rate boundary.

The error bars were calculated for 95% confidence interval, using the method described in the literature.¹⁷ Most of the observed values fall within the 95% confidence interval, which shows that the model derived is quite adequate in predicting the expected conversion.

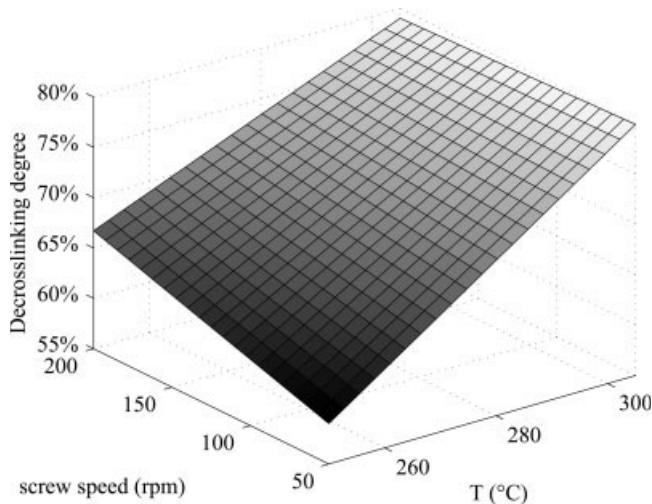


Figure 4 Plot of the decrosslinking degree as a function of screw speed and temperature at low flow rate (3 kg/h).

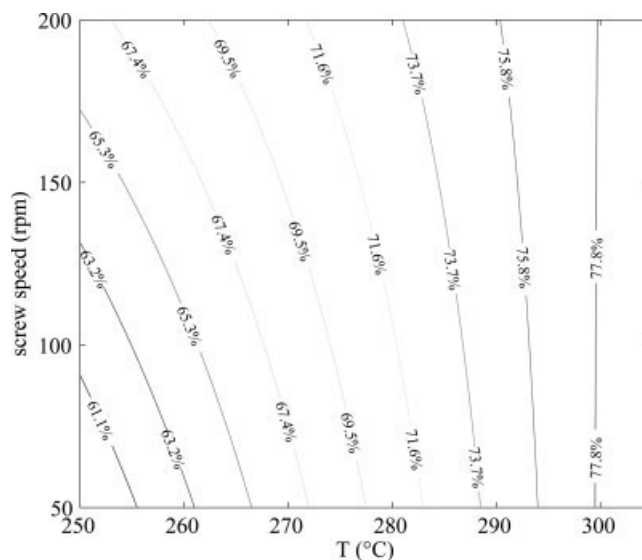


Figure 5 Contour plot of the decrosslinking degree as a function of screw speed and temperature.

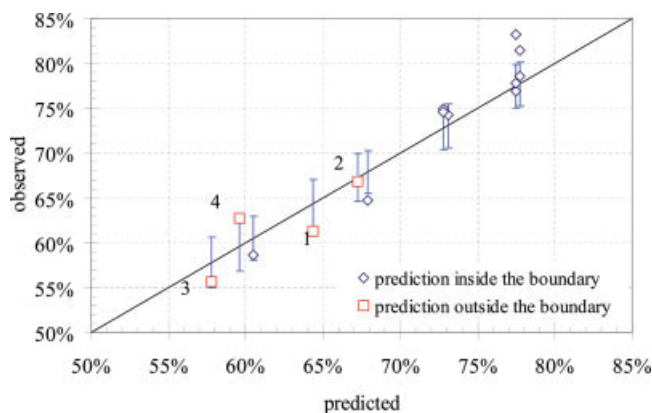


Figure 6 Validation of the decrosslinking degree model. [Color figure can be viewed in the online issue, which is available at www.interscience.wiley.com.]

The graph shows a nice agreement between the measured degrees of decrosslinking with the values calculated by the statistical model. This means that the surface response of the model is quite representative for the process studied.

EPDM ROOFING SHEET

The statistical method was also applied to another EPDM material, namely an EPDM roofing sheet material from Hertel B.V., to see if the process can also be represented by a statistical model in the range studied.

Experimental design

The result from the screening experiments on the roofing sheet material has shown that this rubber is much easier to devulcanize than the profile material. The roofing sheet is readily devulcanized at lower temperature, lower amine concentration, and within shorter residence time compared with the profile material.

Since there was an indication that lower amine concentration can also be used, which is an advantage from the economical point of view, the amine concentration was also varied and therefore four factors were considered in the full factorial design.

TABLE V
Experimental Conditions for Data Points 1–4 in Figure 5

| Experiment | Flow rate (kg/h) | Screw speed (rpm) | Temperature (°C) |
|------------|------------------|-------------------|------------------|
| 1 | 2 | 50 | 250 |
| 2 | 2 | 200 | 250 |
| 3 | 10 | 100 | 250 |
| 4 | 10 | 100 | 270 |

TABLE VI
Settings for Full Factorial Design

| Parameter | Code | High (1) | Low (-1) |
|---------------------|------|----------|----------|
| Temperature (°C) | A | 270 | 230 |
| Feed rate (kg/h) | B | 10 | 3 |
| HDA (mol/kg rubber) | C | 0.3 | 0.1 |
| Screw speed (rpm) | D | 250 | 50 |

A statistical model in eq. (3) is built for the four input variables:¹⁷ temperature (A), feed rate (B), amine concentration (C), and screw speed (D).

$$\begin{aligned} \text{Degree of decrosslinking} = & f_a A + f_b B + f_c C + f_d D \\ & + f_{ab} AB + f_{ac} AC + f_{ad} AD + f_{bc} BC + f_{bd} BD \\ & + \text{Intercept} \pm \text{Error} \quad (3) \end{aligned}$$

The model was limited only to two-parameter interactions, since interactions of more than two parameters are not much useful in practice. The number of combinations needed for a full factorial design for four variables is $2^4 = 16$ experiments. The variables are set either to their high value (coded as 1) or low value (coded as -1) as listed in Table VI. A total of 32 experiments were performed to test the 16 combinations in duplo.

Results and discussion

Analysis of variance and regression model

Decrosslinking degree was calculated as in eq. (2). The ANOVA shows probability (*P*) values lower than 0.05% for all the main factors (*T*, Flow, HDA, and RPM), and the Flow × HDA and Flow × RPM interactions, which means that these factors are significant and they should be included in the model.

Table VII lists the values of the coefficients in eq. (3) for the significant factors (according to the ANOVA), while Figure 7 shows the plot of the model-calculated values versus the observed values, resulting in an R^2 value of 0.96. According to this value, 96% of the variation in the decrosslinking degree can be explained by the model.

TABLE VII
List of the Coefficient Values in Eq. (3)

| | Value |
|----------------------------------|------------------------|
| Intercept | 0.2501 |
| T (°C), f_a | 0.001015 |
| Flow rate (kg/h), f_b | 0.01134 |
| HDA (mol/kg), f_c | 0.4796 |
| Screw speed (rpm), f_d | $3.782 \cdot 10^{-4}$ |
| Flowrate × HDA, f_{bc} | -0.02508 |
| Flowrate × Screw speed, f_{bd} | $-2.882 \cdot 10^{-5}$ |
| Error (+/-) | 0.0018 |

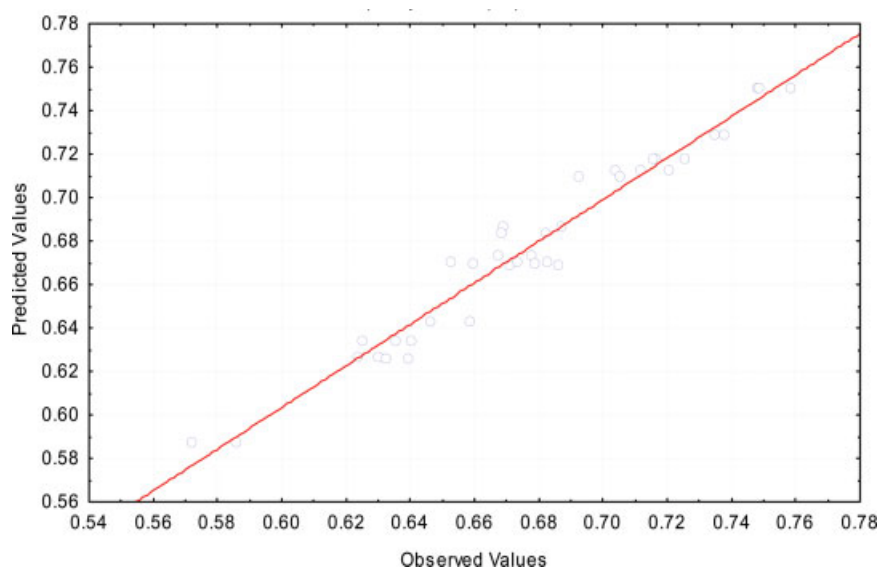


Figure 7 Predicted versus experimental values plot. [Color figure can be viewed in the online issue, which is available at www.interscience.wiley.com.]

In the range studied, the decrosslinking degree is dependent on all of the main factors. Again, the maximum decrosslinking degree was found at the boundary of the range investigated. A maximum conversion of 75.2% was obtained at 250 rpm, 270°C, 0.3 mol HDA/kg rubber, and 3 kg/h rubber flow rate.

Using the statistical model derived, various graphs can be plotted according to the process design requirements as in Figures 8–10. Figure 8 shows the surface response at high flow rate (10 kg/h) and low HDA concentration ([HDA] = 0.1 mol/kg rubber) to determine which temperature and rotation speed should be applied to obtain a certain degree of conversion (decrosslinking). These conditions apply when a high production capacity with a low material (HDA) cost is desired. A higher decrosslinking

degree can be achieved by increasing the temperature, which agrees with the common tendency since a higher temperature provides more thermal energy to overcome the activation energy of the reaction. A high screw speed leads to a higher conversion as it provides higher shear stress, and consequently a higher mechanical energy to break the rubber network.

Figure 9 shows the surface response as a function of screw speed and rubber feed rate, when the temperature is set at its low value (230°C) and low amine concentration is used (0.1 mol HDA/kg rubber). These conditions apply when low operating cost (low heat supply) and low material cost are desired. The surface response shows a nice result since the high conversion (decrosslinking degree) is obtained at high capacity (flow rate), which is an advantage

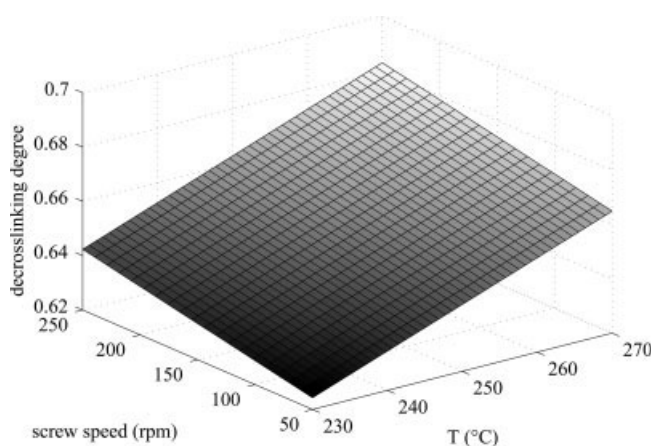


Figure 8 Surface response of the model at high flow rate (10 kg/h) and low HDA concentration (0.1 mol HDA/kg rubber).

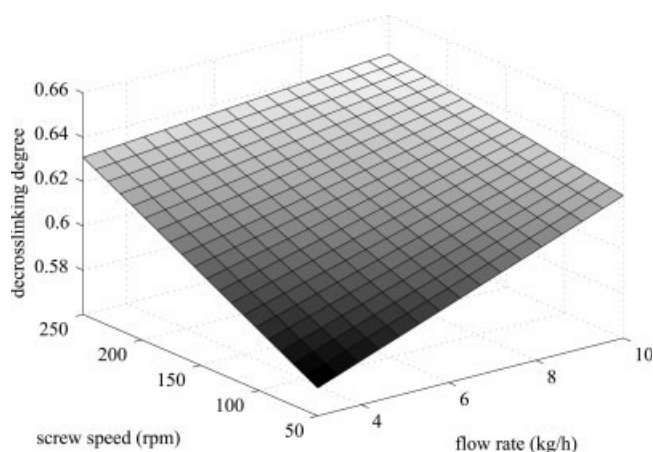


Figure 9 Surface response of the model at low devulcanization temperature (230°C) and low HDA concentration (0.1 mol HDA/kg rubber).

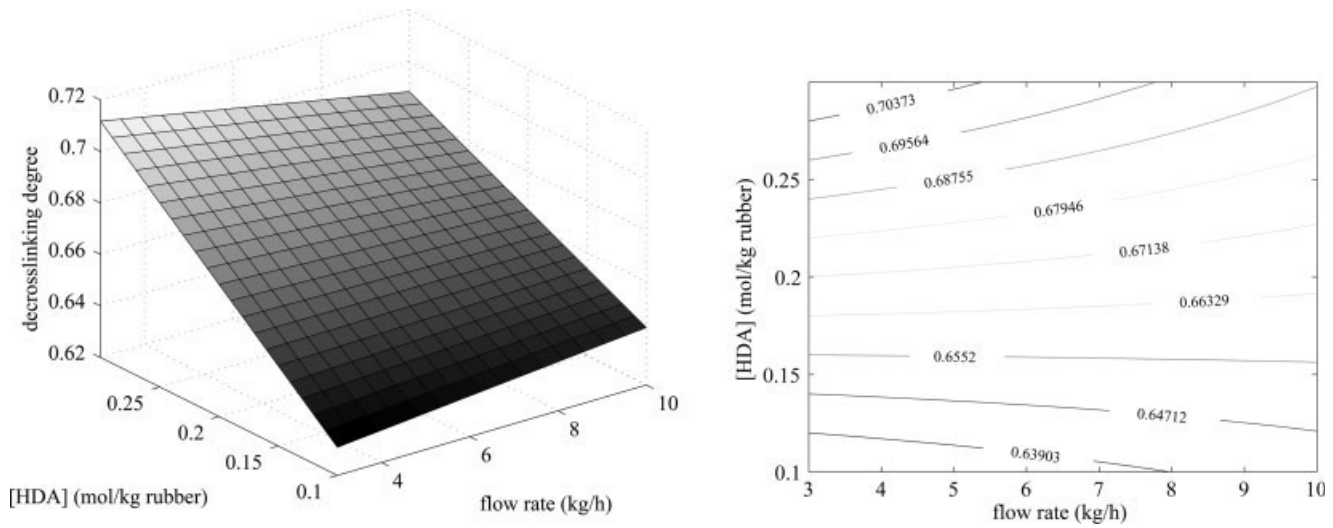


Figure 10 Surface response and contour plot at high screw speed (250 rpm) and low temperature (230°C).

for industrial purpose. The screw speed again indicates the shear rate applied, a higher shear rate results in a further network breakage (conversion).

Figure 9 also shows that the effect of screw speed is more significant at low flow rate than at high flow rate, and that the conversion increases with the flow rate. Both the flow rate and the screw speed influence the specific mechanical energy (*SME*), which is the mechanical energy applied per material mass in the extruder. The *SME* is proportional to the shear rate and inversely proportional to the flow rate,¹⁸ as defined in the following equation

$$SME = \frac{\text{Torque} \cdot 2\pi N}{\dot{M}} \quad (4)$$

where \dot{M} is the mass flow rate and N is the screw speed. The equation for the torque is as follows:¹⁹

$$\text{Torque} = \tau AR(\mu\dot{\gamma})(\pi D_e L)R \quad (5)$$

where τ is the shear stress and equal to $\mu\dot{\gamma}$ for Newtonian liquid, and R is the radius of the screw. A in eq. (5) is the surface on which the shear stress is acting, which in case of an extrusion process is the

barrel surface in the fully filled zone, and is calculated using the effective barrel diameter as described by Booy.²⁰ The L in eq. (5) is the fully filled length, where the shear takes place effectively, and its value is influenced by two factors: the ratio between the feed rate and the drag flow capacity (Q/Q_D), and the length of the pressure build up zone in the extruder end, which is also a function of feed rate Q . A larger value of Q thus results in a larger L . Thus, the flow rate affects the *SME* negatively (due to the larger \dot{M} value) and positively (due to the larger L). In the case with this roofing sheet material, the latter seems to dominate over the former.

A bend on the surface response is observed when setting the screw speed at high value (250 rpm). The response at this condition and low temperature is showed in Figure 10 as a 3-D plot and contour plot. The contour plot gives a very convenient reading in determining the proper [HDA] and flow rate to obtain a certain decrosslinking degree. The 3-D plot gives a better overview of the response behavior at various conditions.

In this case, the 3-D plot shows a different tendency at high [HDA] and low [HDA]. Increasing the flow rate at low [HDA] will slightly increase the

TABLE VIII
Experimental Conditions for Validation Experiments

| Experiment | Flow rate (kg/h) | Screw speed (rpm) | Temperature (°C) | Amine feed (mol/kg) |
|------------|------------------|-------------------|------------------|---------------------|
| 1 | 10 | 100 | 270 | 0.3 |
| 2 | 10 | 250 | 270 | 0.3 |
| 3 | 5 | 250 | 270 | 0.15 |
| 4 | 5 | 250 | 250 | 0.3 |
| 5 | 6 | 200 | 240 | 0.25 |
| 6 | 9 | 150 | 240 | 0.16 |
| 7 | 3 | 200 | 260 | 0.29 |

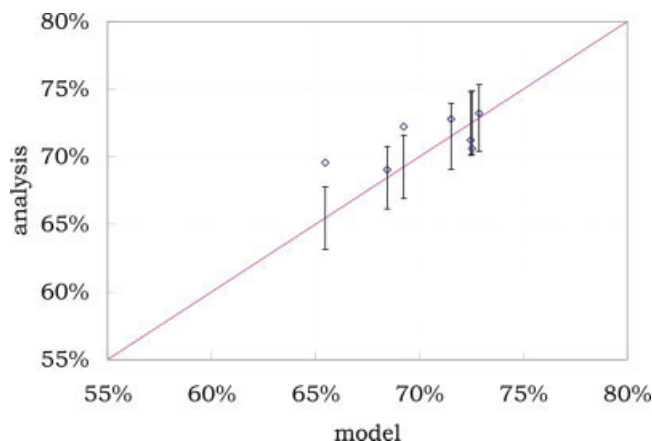


Figure 11 Validation of the decrosslinking degree model. [Color figure can be viewed in the online issue, which is available at www.interscience.wiley.com.]

decrosslinking degree, while increasing it at high [HDA] will decrease the decrosslinking degree. This might be due to the competition between the mechanical and chemical breakage. Apparently, at high concentration of HDA, the chemical breakage plays the main role, which is caused by the higher chemical reaction rate at higher reactant concentrations for a nonzero kinetic order. The residence time at higher flow rate is lower, giving shorter time for the chemical reaction to take place. On the other hand, the mechanical breakage seems to play an important role at low concentration of HDA, especially when (almost) all of the HDA is consumed. This has been proven by the analysis on the HDA remaining in the rubber, which showed that there was almost no HDA left in the devulcanizate when low [HDA] was used. Hence, the conversion at this condition is then influenced by the SME, as has been discussed above.

Model validation

The next step of the statistical modeling is checking if the model can predict the decrosslinking degree at different settings, within the range studied (Table VIII). Figure 11 plots the observed conversions against the predicted values for seven new experiments. The

error bars were calculated for 95% confidence interval according to Ref. 17. Again, most of the observed values fall within this interval, showing that the model is quite adequate in predicting the conversion.

COMPARISONS OF THE TWO MODELS

In general, both models show a similar tendency regarding the temperature and shear rate effects: the conversion is higher at higher temperature and higher shear rate, which is in agreement with the devulcanization model derived in a batch setup.¹⁴

A slight difference is observed in the effect of flow rate on the conversion. A lower flow rate results in a higher conversion in case of EPDM profile material, while the effect is the other way around with EPDM roofing sheet, except at high [HDA] as has been discussed above. This might be explained by the difference in the devulcanization rates of the two rubbers. As it has been observed, even during the screening experiments, the EPDM profile is more difficult to devulcanize. The devulcanization of EPDM profile requires more extreme conditions (higher temperature, longer time, and higher [HDA]) compared to that of the roofing sheet. Since the roofing sheet is much easier to be devulcanized, its melt/solid ratio in the extruder is expected to be higher than that of the EPDM profile. In case of EPDM profile, the rubber just starts melting in the end section of the extruder, while the rubber is still in solid form in most of the extruder length. This melt/solid ratio in the extruder affects the maximum drag capacity Q_D , and in turn influences the degree of fill in the transporting elements, consequently L in eq. (5). The maximum drag capacity Q_D for solid transport is calculated based on the assumption that the particles do not adhere to the channel walls and thus the velocity is equal to that of the screw flight in the axis direction, as given in the following equation

$$Q_{D,\max,\text{solid}} = A_x t_s N \quad (6)$$

On the other hand, the drag capacity of the melt is calculated based on the assumption of laminar

TABLE IX
Torque Data of EPDM Profile at Steady State

| Screw speed and temperature | Flow rate (kg/h) | Relative torque (% from maximum) | % Increase in torque / % Increase in flow rate |
|-----------------------------|------------------|----------------------------------|------------------------------------------------|
| 200 rpm, 300°C | 3 | 14 | 0 |
| | 7 | 14 | |
| 50 rpm, 300°C | 3 | 36 | 1.7 |
| | 7 | 40 | |
| 200 rpm, 250°C | 3 | 12 | 3 |
| | 7 | 19 | |
| 50 rpm, 250°C | 3 | 31 | 3.2 |
| | 7 | 38.5 | |

TABLE X
Torque Data of EPDM Roofing Sheet at Steady State

| Screw speed, temperature, [HDA] | Flow rate (kg/h) | Relative torque (% from maximum) | $\frac{\% \text{ Increase in torque}}{\% \text{ Increase in flow rate}}$ |
|---------------------------------|------------------|----------------------------------|--------------------------------------------------------------------------|
| 100 rpm, 230°C, 0.1 mol/kg | 3 | 17 | 9 |
| | 10 | 47 | |
| 100 rpm, 270°C, 0.1 mol/kg | 3 | 28 | 10.5 |
| | 10 | 63 | |
| 250 rpm, 270°C, 0.1 mol/kg | 3 | 12 | 13.2 |
| | 10 | 56 | |
| 250 rpm, 230°C, 0.3 mol/kg | 3 | 12 | 10.2 |
| | 10 | 46 | |

flow, where the average velocity is half of the wall velocity:²¹

$$Q_{D,\max,\text{melt}} = 0.5mHW(\pi ND_s) \cos \varphi f_D \quad (7)$$

When the density of the material is similar in its solid and melt form, which is the case here, the Q_D for the melt flow is thus about the half of that of the solid flow. Considering that L is proportional to the ratio of Q/Q_D , the L in solid flow is thus less influenced by the flow rate Q when Q_D is larger. The same effect also applies in the length of the pressure build up zone before the extruder die. Hence, the fully filled volume in the extruder is more affected by the flow rate in case of the EPDM roofing sheet devulcanization, while its value can nearly be assumed constant in case of EPDM profile material. Subsequently, the positive effect of the flow rate in case of the EPDM roofing sheet is significant, while that of the EPDM profile is negligible.

The hypothesis above is supported by the collected torque data listed in Tables IX and X. The table shows the torque value at similar temperature and rotation speed, at different flow rates. The table shows a negligible influence of flow rate on the torque for EPDM profile (calculated as % increase in torque divided by % increase in flow rate), while the influence is significant for EPDM roofing sheet.

CONCLUSIONS

The model obtained represents the data satisfactorily within the boundaries studied. Nevertheless, extending the model to predict the result of the process at points outside the boundaries needs extra attention.

Screening experiments and the knowledge of extrusion principles facilitate the understanding of the responses. The responses of the statistical models derived here can be nicely explained by general extruder theories and the knowledge of the influence of the involved parameters on the devulcanization.

The process responses of both EPDM materials studied here show similar tendency with temperature and screw speed (shear). Anyhow, as it has been

shown here, the devulcanizations of different EPDM compounds might show different tendencies in their responses. When the material is easily devulcanized, the influence of flow rate on the degree of fill in the extruder (and hence, the conversion) is more significant, which can be explained by extrusion theory.

NOMENCLATURE

| | |
|-----------------------------------|------------------------------------------------------------------------------------------------|
| A_x (m ²) | the cross-sectional area of the gap between the screw and the barrel according to Refs. 20, 22 |
| DoF | degrees of freedom |
| f | Coefficient of each factor or of their interaction |
| f_D | Geometrical correction factor for drag flow |
| H (m) | height of the channel |
| [HDA] | |
| (mol/g rubber) | hexadecylamine concentration |
| L (m) | fully filled length of the extruder |
| M | number of parallel channels |
| \dot{M} (kg/s) | mass flow rate |
| MS | mean square |
| N (rps) | rotation speed |
| Q (m ³ /s) | volumetric flow rate |
| $Q_{D,\max}$ (m ³ /s) | maximum drag flow capacity |
| R (m) | screw radius |
| SS | sum of squares |
| t_s (m) | screw lead \equiv the axial displacement caused by one rotation |
| W (m) | width of the channel |
| XL (mol/g rubber) | crosslink density |
| $\dot{\gamma}$ (s ⁻¹) | shear rate |
| μ (Pa s) | viscosity |
| φ (rad) | helix angle at R |
| τ (Pa) | shear stress |

References

1. Report, International Institute of Synthetic Rubber Producers, 2003.
2. Noordermeer, J. W. M. In Kirk-Othmer Concise Encyclopedia of Chemical Technology; Kirk, R. E.; Othmer, D. F.; Grayson, M., Eds.; Wiley-Interscience: New York, 1993; Vol. 8.

3. Burrige, E. EPDM. *Eur Chem News* 2003, 10–16, 15.
4. Burrige, E. EPDM. *Eur Chem News* 2005, 82, 16.
5. Yun, J.; Yashin, V. V.; Isayev, A. I. In *Rubber Division Meeting, American Chemical Society, Pittsburgh, October 8–11, 2002*; Paper No. 118.
6. Yun, J.; Isayev, A. I. *Polym Eng Sci* 2003, 43, 809.
7. Yun, J.; Yashin, V. V.; Isayev, A. I. *J Appl Polym Sci* 2004, 91, 1646.
8. Mouri, M.; Okamoto, H.; Matsushita, M.; Honda, H.; Nakashima, K.; Takeushi, K.; Suzuki, Y.; Owaki, M. *Int Polym Sci Tech* 2000, 27, T/23.
9. Mouri, M.; Sato, N.; Okamoto, H.; Matsushita, M.; Honda, H.; Nakashima, K.; Takeushi, K.; Suzuki, Y.; Owaki, M. *Int Polym Sci Tech* 2000, 27, T/17.
10. Mouri, M.; Sato, N.; Okamoto, H.; Matsushita, M.; Honda, H.; Nakashima, K.; Suzuki, Y.; Owaki, M. *Int Polym Sci Tech* 2000, 27, T/12.
11. Sato, N. In *International Rubber Conference (IRC) Proceeding, Seoul, Korea, 1999*.
12. Suzuki, Y.; Owaki, M.; Mouri, M.; Sato, N.; Honda, H.; Nakashima, K. *Toyota Tech Rev* 1998, 48, 53.
13. van Duin, M.; Noordermeer, J. W. M.; Verbruggen, M. A. L.; van der Does, L. *Method for Devulcanizing Rubber with an Amine*, US Patent 2,003,013,776, 2003. the Netherlands.
14. Sutanto, P.; Laksana, F.; Picchioni, F.; Janssen, L. P. B. M. *Chem Eng Sci* 2006, 61, 6442.
15. Sutanto, P.; Picchioni, F.; Janssen, L. P. B. M. *Chem Eng Sci*, to appear.
16. Flory, P. J. *J Chem Phys* 1950, 18, 108.
17. Montgomery, D. C., Ed. *Design and Analysis of Experiments*, 5th ed.; Wiley: New York, 2001.
18. Chang, Y. K.; Martinez-Bustos, F.; Park, T. S.; Kokini, J. L. *Braz J Chem Eng* 1999, 16, 285.
19. Bird, R. B.; Stewart, W. E.; Lightfoot, E. N. *Transport Phenomena*; Wiley: New York, 1994.
20. Booy, M. L. *Polym Eng Sci* 1978, 18, 973.
21. Rauwendaal, C., Ed. *Polymer Extrusion*, 3rd ed.; Hanser: Germany, 1994.
22. Booy, M. L. *Polym Eng Sci* 1980, 20, 1220.